A Projection Method for Constructing a Mass Conservative Velocity Field

by

S. Chippada
C. N. Dawson
M. L. Martinez
M. F. Wheeler

DoD HPC Modernization Program
Programming Environment and Training

CEWES MSRC

CEWES
MSRC

Nichols
Research

04h01298

A Projection Method for Constructing a Mass Conservative Velocity Field [*],[**]

S. Chippada, C. N. Dawson, M. L. Martínez, M. F. Wheeler

Center for Subsurface Modeling
Texas Institute for Computational and Applied Mathematics
University of Texas, Austin, TX 78712, USA.

Abstract

In the numerical modeling of fluid flow and transport problems frequently the velocity field needs to be projected from one finite dimensional space into another. In certain applications, especially those involving modeling of multi-species transport, the new projected velocity field should be accurate as well as locally mass conservative.

In this paper, a velocity projection method has been developed that is both accurate and mass conservative element-by-element on the projected grid. The velocity correction is expressed as gradient of a scalar pressure field, and the resultant Poisson equation is solved using a mixed/hybrid finite element method and lowest-order Raviart Thomas spaces. The conservative projection method is applied to the system of shallow water equations and a theoretical error estimate is derived.

1 Introduction

In the numerical modeling of fluid flow and transport problems, the computed velocity field frequently needs to be projected from one finite dimensional subspace into another, possibly to satisfy some constraint or because the underlying mesh has changed. For example, in Lagrangian-based numerical modeling of free boundary problems, to avoid mesh distortions the numerical mesh is regenerated once every few time steps, and in such situations the velocity field

has to be projected from the old grid onto the new grid. Other important applications where the velocity field may need to be projected are in the modeling of environmental surface and subsurface flow and transport problems. In these problems, the flow and transport equations arise from conservation of mass (plus some additional equations such as Darcy's Law or the Navier-Stokes equations). The flow and multi-species transport are often solved separately using completely different numerical methods and grids due to differences in length and time scales of the phenomena involved. For accurate transport, it is desirable for the velocities to be locally conservative on the transport grid. This can be accomplished through the projection algorithm described below.

A particular example on which we will focus is the modeling of surface flow. Here the flow model is described by the shallow water equations. The ADCIRC (an advanced circulation model for shelves, coasts and estuaries) (Lynch and Gray, 1979; Luettich, Westerink and Scheffner, 1991) and RMA codes (King and Norton, 1978) are examples of widely used shallow water hydrodynamics models. Both models are based on Galerkin-type finite element methods and unstructured triangular grids. The velocities computed with these models can serve as input to a multi-species transport model. For example, the CE-QUAL-ICM (Cerco and Cole, 1996) simulator is a widely used water quality model. It uses unstructured quadrilateral grids and finite volume type discretization. All of these codes are utilized by U.S. Army Corps of Engineers at the Waterways Experiment Station in Vicksburg, Mississippi, and other state and federal agencies in modeling environmental quality of shallow water systems. Therefore, there is a need to couple these hydrodynamic and water quality models and to perform a projection to produce a locally conservative velocity field on the transport grid.

In this paper we present an approach which we call the *conservative velocity projection method*, which projects a computed velocity field from one finite dimensional space into another in an accurate and element-by-element mass conservative manner. In particular, we will focus on a projection algorithm based on the mixed/hybrid finite element method. This method is well-suited for computing locally conservative velocity fields.

In §2, the mathematical aspects of hydrodynamics and environmental modeling are briefly discussed. The conservative projection method and the mixed/hybrid finite element method are outlined in §3. An error estimate for the accuracy of the projected velocity field is derived in §4. The application of the projection method to the shallow water equations modeled using the ADCIRC code is presented in §5. Finally, in §6, we conclude with some remarks and future research possibilities.

2 Flow and Transport Modeling

The most general form of the conservation of mass equation is given by:

$$\frac{\partial \rho}{\partial t} + \boldsymbol{\nabla} \cdot \mathbf{U} = q. \tag{1}$$

In the above equation, ρ is the the fluid density, $\mathbf{u}$ is the velocity vector field, $\mathbf{U} = \rho\mathbf{u}$, $\boldsymbol{\nabla}$ is the spatial gradient operator and q represents the sources and sinks that may be present in the flow domain. In most hydrodynamics situations the fluid flow is incompressible and the mass conservation equation simplifies to:

$$\boldsymbol{\nabla} \cdot \mathbf{u} = q. \tag{2}$$

We present the projection method for a fluid flow system with conservation of mass of the form given by Eq.1, but the procedure and analysis carries forward in a straight forward manner to the case of incompressible flows also. Further, in the case of shallow water systems, even though the fluid flow is governed by the 3-D incompressible Navier-Stokes equations, after depth-averaging we obtain a mathematical system which is compressible in nature with conservation of mass equation of the form given by Eq.1 and the fluid depth H playing the role of density.

The fluid flow mathematical model typically consists of a mass conservation equation given by either Eq.1 or Eq.2 and a momentum conservation law. Several forms of momentum conservation laws are used depending on the flow situations. In high-speed aerodynamic flows compressible Navier-Stokes equations are used whereas in the case of low speed hydraulic flows the incompressible Navier-Stokes equations are solved. In the case of flow through porous media the velocity field is determined using Darcy's law. In certain flow problems the energy equation and an equation of state may also have to be solved simultaneously along with the mass and momentum equations. The actual form of the fluid flow model itself is not important since in this paper we are only interested in post-processing a given fluid flow field so that it is locally mass-conservative on the same grid or on an entirely new grid. As proof-of-concept, we apply the conservative velocity projection method to the fluid flow governed by the system of shallow water equations and this hydrodynamics model is described in detail in §5.

We assume that we have a hydrodynamics model governing the fluid flow consisting of a mass conservation law (Eq.1) and a momentum conservation law and any other equations that may be necessary to compute the flow field.

This system is numerically solved using any of the existing finite difference, finite element and finite volume type numerical schemes.

The multi-species transport model consists of a system of advection-diffusion-reaction type transport equations of the following form:

$$\frac{\partial \left(\rho c_i\right)}{\partial t} + \boldsymbol{\nabla} \cdot \left(\rho \mathbf{u} c_i\right) = \boldsymbol{\nabla} \cdot \left(D_i \boldsymbol{\nabla} c_i\right) + q c_i + R_i, \quad i = 1 \cdots N, \quad (3)$$

where c_i is the concentration per unit mass of species i, R_i is a reaction-type source function and D_i is the diffusion coefficient. The primary influence of the flow field is in the advective transport of the concentration species. In case of turbulent fluid flows the velocity field can also influence the diffusion coefficient D_i. Here we are assuming passive scalar transport and that the concentration field doesn't affect the fluid flow. If this is not the case then we need to solve the hydrodynamics and concentration equations together preferably on the same grids.

In the numerical solution of the concentration equations it is important that the velocity field be mass conservative cell-by-cell. This can be seen more clearly if we rewrite the transport equation (Eq.3) in the following way:

$$\rho \left(\frac{\partial c_i}{\partial t} + \mathbf{u} \cdot \boldsymbol{\nabla} c_i - \frac{1}{\rho} \boldsymbol{\nabla} \cdot \left(D_i \boldsymbol{\nabla} c_i\right) - \frac{1}{\rho} R_i\right) + c_i \left(\frac{\partial \rho}{\partial t} + \boldsymbol{\nabla} \cdot \left(\rho \mathbf{u}\right) - q\right) = 0. \quad (4)$$

The mass conservation equation is present in the species transport equation (Eq.3), and if we do not have local mass conservation it amounts to adding spurious sources and sinks. This could give rise to numerical instabilities, especially if we are interested in integrating the equations over long periods of time. Also, in some applications the concentrations are very small (of the order of 10^{-6}) and small errors in mass conservation can have significant influence on the accuracy and stability of the system. Thus, it is important for the velocity field to be cell-by-cell mass conservative in the multi-species transport studies.

3 Conservative Projection Formulation

Let $\Omega \in R^n$, n = 2 or 3, be the physical domain and $\partial \Omega$ the external boundary of this domain. Further, let $\partial \Omega_1$ be the boundary on which we have Dirichlet boundary conditions on the normal velocity expressed as:

$$\mathbf{U} \cdot \boldsymbol{\nu} = g \quad \text{on} \quad \partial \Omega_1, \quad (5)$$

where $\boldsymbol{\nu}$ is the outward pointing unit normal vector at the boundary. Let h^o be the mesh parameter of the old grid and h^n be the mesh parameter of the new grid. Further, let $\bar{\mathbf{V}}_{h^o}$ and $\mathbf{V}_{h^n}$ be finite dimensional subspaces corresponding to the old and new meshes. Given $\mathbf{U}_{h^o} \in \bar{\mathbf{V}}_{h^o}$ the problem is to find $\mathbf{U}_{h^n} \in \mathbf{V}_{h^n}$ such that $\mathbf{U}_{h^n}$ is a close approximation of $\mathbf{U}_{h^o}$ and that $\mathbf{U}_{h^n}$ "satisfies" the mass conservation law given by:

$$\nabla \cdot \mathbf{U}_{h^n} = q - \frac{\partial \rho}{\partial t} = f \quad \text{in} \ \ \Omega, \ \ \text{and}$$
$$\mathbf{U}_{h^n} \cdot \boldsymbol{\nu} = g \qquad \qquad \text{on} \ \ \partial\Omega_1. \tag{6}$$

The new velocity $\mathbf{U}_{h^n}$ is expressed in terms of the old velocity $\mathbf{U}_{h^o}$ in the following manner:

$$\mathbf{U}_{h^n} = \mathcal{P}_{h^n} \mathbf{U}_{h^o} + \boldsymbol{\Gamma}_{h^n} \quad \in \mathbf{V}_{h^n}, \tag{7}$$

where $\mathcal{P}_{h^n} \mathbf{U}_{h^o}$ is the $\mathcal{L}^2$ projection of the old velocity $\mathbf{U}_{h^o}$ into $\mathbf{V}_{h^n}$ and $,_{h^n} \in \mathbf{V}_{h^n}$ is the velocity correction which we need to compute. Substituting Eq.7 into Eq.6 we obtain the following boundary value problem:

$$\nabla \cdot \boldsymbol{\Gamma}_{h^n} = \mathrm{f} - \nabla \cdot \mathcal{P}_{h^n} \mathbf{U}_{h^o} = \tilde{\mathrm{f}} \quad \text{in} \ \ \Omega, \ \ \text{and}$$
$$\boldsymbol{\Gamma}_{h^n} \cdot \boldsymbol{\nu} = \mathrm{g} - \mathcal{P}_{h^n} \mathbf{U}_{h^o} \cdot \boldsymbol{\nu} = \tilde{\mathrm{g}} \quad \text{on} \ \ \partial\Omega_1. \tag{8}$$

Further, we express $\boldsymbol{\Gamma}_{h^n}$ as the gradient of a scalar function in the following manner:

$$\boldsymbol{\Gamma}_{h^n} = -\nabla \phi_{h^n}. \tag{9}$$

The scalar variable ϕ_{h^n} can be thought of as a pseudo-pressure. This type of representation implies that the vorticity of the new velocity field $\mathbf{U}_{h^n}$ is same as that of the old velocity field $\mathcal{P}_{h^n} \mathbf{U}_{h^o}$ and the velocity correction $,_{h^n}$ helps us obtain local mass conservation without changing the vorticity of the velocity field. Substituting Eq.9 into Eq.8 we obtain the following elliptic problem:

$$-\triangle \phi_{h^n} = \tilde{\mathrm{f}} \qquad \text{on} \ \ \Omega,$$
$$-\nabla \phi_h \cdot \boldsymbol{\nu} = \tilde{\mathrm{g}} \qquad \text{on} \ \ \partial\Omega_1, and$$
$$\phi_{h^n} = 0 \qquad \text{on} \ \ \partial\Omega / \partial\Omega_1. \tag{10}$$

The elliptic problem given by Eq.10 is solved using the mixed/hybrid finite element method which approximates both fluxes ($\boldsymbol{\Gamma}$) and pressures (ϕ).
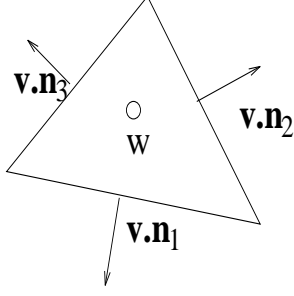
Fig. 1. Piece-wise approximations on a triangular element using lowest-order Raviart-Thomas spaces.

In addition, the fluxes $\mathbf{\Gamma}{\cdot}\boldsymbol{\nu} = -\boldsymbol{\nabla}\phi{\cdot}\boldsymbol{\nu}$ are continuous across the edges and the resulting numerical solution satisfies mass conservation cell-by-cell. The mixed/hybrid finite element approximation of the elliptic problem (Eq.10) together with velocity relations (Eqs.7 and 9) represent the *conservative velocity projection formulation.*

On the new grid, the elliptic problem is approximated using triangular elements and lowest-order Raviart-Thomas spaces which are written as follows for a given triangular element E (see Fig.1):

$$\mathrm{W}_{h^n}(\mathrm{E}) = \{a \in \mathrm{R} \quad \mathrm{on} \quad \mathrm{E}\}, \quad \mathrm{and} \tag{11}$$

$$\mathbf{V}_{h^n}(\mathrm{E}) = \begin{pmatrix} \alpha + \beta\mathrm{x} \\ \gamma + \beta\mathrm{y} \end{pmatrix}; \quad \alpha, \beta, \gamma \in \mathrm{R}, \quad (\mathrm{x}, \mathrm{y}) \in \mathrm{E}. \tag{12}$$

The finite dimensional scalar and vector spaces on the new grid are defined as:

$$\mathrm{W}_{h^n} = \left\{ w \in \mathcal{L}^2(\Omega) : w|_{\mathrm{E}} \in \mathrm{W}_{h^n}(\mathrm{E}) \forall \mathrm{E} \right\} \tag{13}$$

$$\mathbf{V}_{h^n} = \left\{ \mathbf{v} \in \mathcal{L}^2(\Omega) : \mathbf{v}|_{\mathrm{E}} \in \mathbf{V}_{h^n}(\mathrm{E}) \forall \mathrm{E} \right\} \tag{14}$$

In the mixed/hybrid finite element method the second-order elliptic problem is written as a first-order system and we compute $(\mathbf{\Gamma}_{h^n}, \phi_{h^n}) \in (\mathbf{V}_{h^n}, W_{h^n})$ from:

$$
\begin{aligned}
(\mathbf{\Gamma}_{h^n}, \mathbf{v}_{h^n}) - (\phi_{h^n}, \boldsymbol{\nabla}{\cdot}\mathbf{v}_{h^n}) &= 0 &\forall \ \mathbf{v}_{h^n} \in \mathbf{V}_{h^n} \\
(\boldsymbol{\nabla}{\cdot}\mathbf{\Gamma}_{h^n}, w_{h^n}) &= \left(\tilde{\mathrm{f}}, w_{h^n}\right) &\forall \ w_{h^n} \in W_{h^n} \\
<\mathbf{\Gamma}_{h^n}{\cdot}\boldsymbol{\nu}, \mathbf{v}_{h^n}{\cdot}\boldsymbol{\nu}> &=<\tilde{\mathrm{g}}, \mathbf{v}_{h^n}{\cdot}\boldsymbol{\nu}> &\forall \ \mathbf{v}_{h^n} \in \mathbf{V}_{h^n}
\end{aligned}
\tag{15}
$$

In the above weak formulation, $(\cdot, \cdot)$ and $< \cdot, \cdot >$ are the the usual inner products on the domain Ω and the boundary $\partial \Omega$, respectively. We refer the reader to Raviart and Thomas (1977) and Brezzi and Fortin (1991) for more information on the mixed/hybrid finite element method and their implementation details.

4 Theoretical Error Estimate

The $\mathcal{L}^2$ projection of $\mathbf{U}_{h^o}$ into $\mathbf{V}_{h^n}$ is defined by

$$((\mathbf{U}_{h^o} - \mathcal{P}_{h^n} \mathbf{U}_{h^o}), \mathbf{v}_{h^n}) = 0, \quad \forall \mathbf{v}_{h^n} \in \mathbf{V}_{h^n}.$$

Also, the $\mathbf{\Pi}_{h^n}$-projection of $\mathbf{U}$ into V_{h^n} is defined by

$$(\mathbf{\nabla} \cdot (\mathbf{U} - \mathbf{\Pi}_{h^n} \mathbf{U}), w_{h^n}) = 0, \quad \forall w_{h^n} \in W_{h^n}.$$

Theorem 4.1 *Given $\mathbf{U}_{h^o}, \mathbf{U}_{h^n}$, $\exists$ a constant C independent of $h^n, h^o, \mathbf{U}$ such that*

$$\|\mathbf{U}_{h^n} - \mathbf{U}\| \leq C \left(\|\mathbf{\Pi}_{h^n} \mathbf{U} - \mathbf{U}\| + \|\mathbf{U}_{h^o} - \mathbf{U}\| \right). \tag{16}$$

Proof: First, write Eq.7 in weak form to get

$$(\mathbf{U}_{h^n}, \mathbf{v}_{h^n}) = (\mathcal{P}_{h^n} \mathbf{U}_{h^o}, \mathbf{v}_{h^n}) + (\mathbf{\Gamma}_{h^n}, \mathbf{v}_{h^n}), \quad \forall \mathbf{v}_{h^n} \in \mathbf{V}_{h^n}. \tag{17}$$

Subtract $(\mathbf{U}, \mathbf{v}_{h^n})$ from both sides of Eq.17 and use the definition of the $\mathcal{L}^2$ projection to get

$$(\mathbf{U}_{h^n} - \mathbf{U}, \mathbf{v}_{h^n}) = (\mathbf{U}_{h^o} - \mathbf{U}, \mathbf{v}_{h^n}) + (\mathbf{\Gamma}_{h^n}, \mathbf{v}_{h^n}), \quad \forall \mathbf{v}_{h^n} \in \mathbf{V}_{h^n}. \tag{18}$$

By choosing $\mathbf{v}_{h^n} = \mathbf{U}_{h^n} - \mathbf{\Pi}_{h^n} \mathbf{U}$, we can reduce to zero the second term in the right hand side of Eq.18. This is accomplished by using our chosen test function in the first relation of Eq.15, together with the definition of the $\mathbf{\Pi}_{h^n}$ projection and the fact that the mass conservation equation is satisfied by both the true velocity $\mathbf{U}$ and the new velocity $\mathbf{U}_{h^n}$.

Finally, manipulate

$$\begin{aligned}
(\mathbf{U}_{h^n} - \mathbf{U}, (\mathbf{U}_{h^n} - \mathbf{U}) &- (\mathbf{\Pi}_{h^n} \mathbf{U} - \mathbf{U})) \\
&= (\mathbf{U}_{h^o} - \mathbf{U}, (\mathbf{U}_{h^n} - \mathbf{U}) - (\mathbf{\Pi}_{h^n} \mathbf{U} - \mathbf{U}))
\end{aligned}$$

using Cauchy-Schwartz and the arithmetic-geometric-mean inequality,

$$ab \leq \frac{1}{4\epsilon}a^2 + \epsilon b^2, \quad \epsilon > 0,$$

to obtain the result of the theorem. $\quad\square$

The elegance of the estimate comes from the observation that it reduces to an approximation theory question given an estimate for the difference between $\mathbf{U}_{h^\circ}$ and the true velocity $\mathbf{U}$.

For example, using the lowest-order Raviart-Thomas space in computing $\mathbf{U}_{h^n}$ (Raviart and Thomas, 1977; Brezzi and Fortin, 1991) and using, say, the AD-CIRC model to compute $\mathbf{U}_{h^\circ}$ (Chippada, Dawson, Martínez and Wheeler, 1995), then $||\mathbf{U}_{h^n} - \mathbf{U}|| \leq Ch$.

5   Application: Shallow Water Equations

The projection formulation developed in §3 is applied to the system of shallow water equations. Shallow water equations (SWE) are obtained through the vertical integration of the 3-D incompressible Navier-Stokes along with assumptions of hydrostatic pressure and vertically uniform velocity profiles (Weiyan, 1992). Due to the assumptions made in their derivation, SWE are valid only for flow systems with horizontal length scales much larger compared to the fluid depth. A typical shallow water system is shown in Fig.2. The conservation of mass in the system of shallow water equations is given by:

$$\mathcal{L} \equiv \frac{\partial \xi}{\partial \mathrm{t}} + \boldsymbol{\nabla} \cdot (\mathbf{u}\mathrm{H}) = 0. \tag{19}$$

The non-conservative form of the momentum equation is as follows:

$$\mathcal{M} \equiv \frac{\partial \mathbf{u}}{\partial \mathrm{t}} + \mathbf{u} \cdot \boldsymbol{\nabla}\mathbf{u} + \mathrm{g}\boldsymbol{\nabla}\xi - \frac{1}{H}\boldsymbol{\nabla} \cdot [H\boldsymbol{\sigma}] + \tau_{bf}\mathbf{u} + f_c\mathbf{k} \times \mathbf{u} - \mathbf{f}_b = 0. \tag{20}$$

In the above system, ξ is the deflection of the air-water interface from the mean sea level (see Fig.3), $\mathrm{H} = \xi + h_b$ is the total fluid depth and h_b is the bathymetric depth. The velocity field is denoted by $\mathbf{u}$ and is the mean velocity across the vertical. $\mathbf{U} = \mathbf{u}H$ is the total flow rate (discharge) and τ_{bf} and f_c are respectively the bottom friction and Coriolis acceleration coefficients; $\boldsymbol{\sigma}$ is the viscous stress tensor and is neglected in most applications since the bottom friction terms dominate the lateral diffusion and dispersion. Several types of
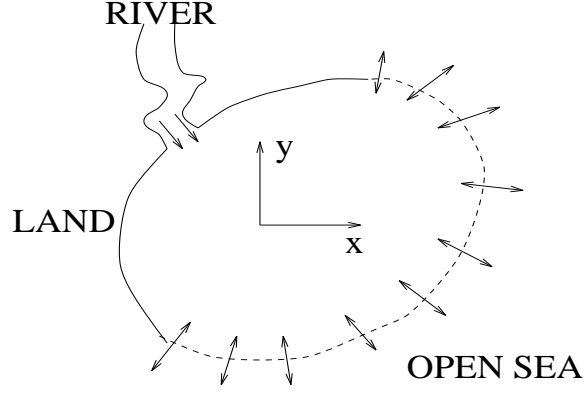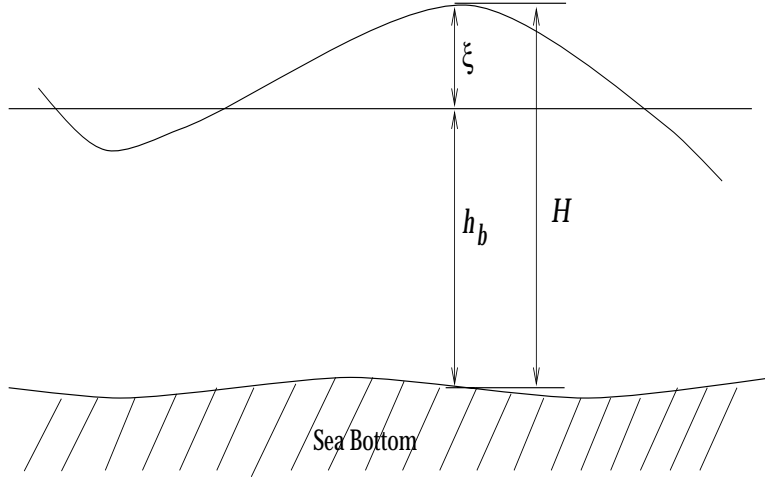
Fig. 2. A typical shallow water system

Fig. 3. Definition of ξ, h_b and H.

body forces act on the system including the wind stress, atmospheric pressure gradient and tidal potential forces and all of these are lumped into the generic body force term $\mathbf{f}_b$. The conservative form of the momentum equation can be derived from Eqs.19 and 20 in the following manner:

$$\mathcal{M}_c \equiv H\mathcal{M} + \mathbf{u}\mathcal{L} = 0 \tag{21}$$

A variety of numerical methods have been developed to solve the system of shallow water equations. Due to the strong coupling between the velocity and elevation fields, if the numerical method is not chosen properly, we could run into the problem of spurious spatial oscillations. Gray, Westerink, Luettich, Kinnmark, Kolar and others [7,8] have developed over the years a numerical procedure (code) called ADCIRC. They replace the first-order mass conservation equation (Eq.19) with a second-order generalized wave continuity

equation (GWCE) which is given by:

$$\mathcal{G} \equiv \frac{\partial L}{\partial \mathrm{t}} - \boldsymbol{\nabla} \cdot \mathcal{M}_c + \tau_0 \mathcal{L} = 0 \tag{22}$$

The resulting form of the GWCE is:

$$\frac{\partial^2 \xi}{\partial \mathrm{t}^2} + \tau_0 \frac{\partial \xi}{\partial \mathrm{t}} + \boldsymbol{\nabla} \cdot [(\tau_0 - \tau_{bf}) H \mathbf{u}]$$
$$- \boldsymbol{\nabla} \cdot [\boldsymbol{\nabla} \cdot (H \mathbf{u}\mathbf{u}) + H f_c \mathbf{k} \times \mathbf{u} + \mathrm{g} H \boldsymbol{\nabla} \xi - \boldsymbol{\nabla} \cdot [H \boldsymbol{\sigma}] - H \mathbf{f}_b] = 0 \tag{23}$$

In the above equation, τ_0 is a numerical parameter which is chosen based on stability and accuracy criteria and is usually $1 - 10$ times the bottom friction coefficient τ_{bf} (Kolar, Gray and Westerink, 1996). The GWCE (Eq.23) along with the non-conservative momentum equation (Eq.20) is solved using the Galerkin finite element method and linear triangular elements. The main advantage of this method is that it lets us choose the same approximating spaces for both the velocities and pressure without giving rise to spurious spatial oscillations. Thus, this approach is numerically very efficient and has been used extensively in the study of many shallow water systems and is one of the hydrodynamics code used by the US Army Corps of Engineers at the Waterways Experiment Station, Vicksburg, Mississippi. The velocity field obtained from this numerical approach is globally mass conservative but mass conservation on the local numerical cell is not guaranteed. We apply the projection formulation outlined in §3 to postprocess this velocity field so that the resulting velocity field is mass conservative cell-by-cell. For simplicity, we assume that the transport grid is same as the hydrodynamics grid.

The physical problem simulated is tidal waves in Galveston Bay. The numerical grid and bathymetry are shown in Figs.4 and 5.

The physical geometry is very complex and there are large variations in the bathymetric depth near the Houston shipping channel. The system is driven by tidal waves which come from the open sea. We start with zero initial elevation deflections and velocity fields, and slowly apply the forcing functions through the use of a hyperbolic tangent ramp function over a period of two days. The simulation is run for twelve days and the elevation distribution and the discharge $\mathbf{U} = \mathbf{u}\mathrm{H}$ at the end of twelve days are shown in Fig.6. The local mass conservation errors are computed on each cell and are plotted in Fig.7. Notice that we have maximum mass conservation errors occurring near and within the Houston Ship Channel as well as near the other inlets. The old velocity field coming from the ADCIRC code are post-processed using the conservative projection formulation described in §3. The resultant pseudo-pressure ϕ and correction velocity $\boldsymbol{\Gamma}$ are shown in Fig.8. The velocity corrections are significant in the areas of maximum mass conservation errors.
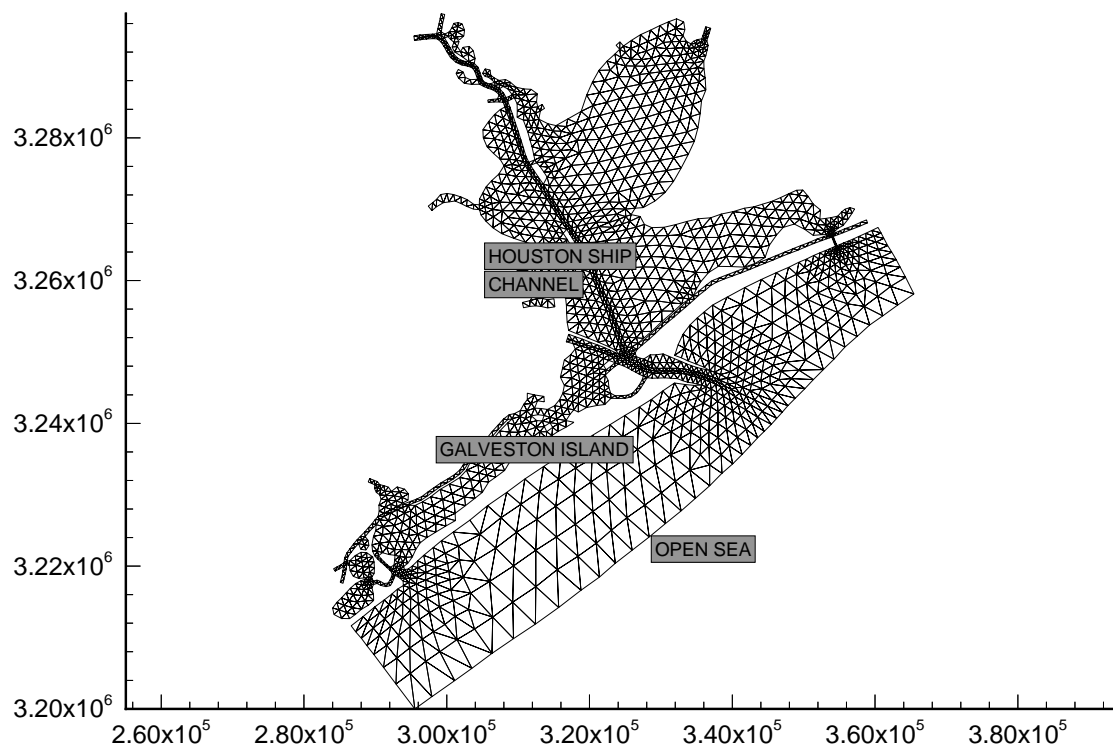
Fig. 4. Galveston Bay: numerical mesh. Lengths shown are in meters.

6   Concluding Remarks and Future Work

A conservative velocity projection scheme that projects the velocity field from one grid onto another in an accurate and locally mass conservative manner has been defined. A theoretical error estimate of the conservative projection formulation has been derived and numerical results pertaining to the system of shallow water equations have been presented. The procedure proposed in this paper is very general and extends readily to 3-D and other general elements. Another advantage of this procedure is that it can be applied only in regions of large mass conservation errors thus giving great computational efficiency.

In the future, we are looking at coupling 3-D ADCIRC velocities with CE-QUAL-ICM. We also plan to investigate the application of this approach to non-matching grids.
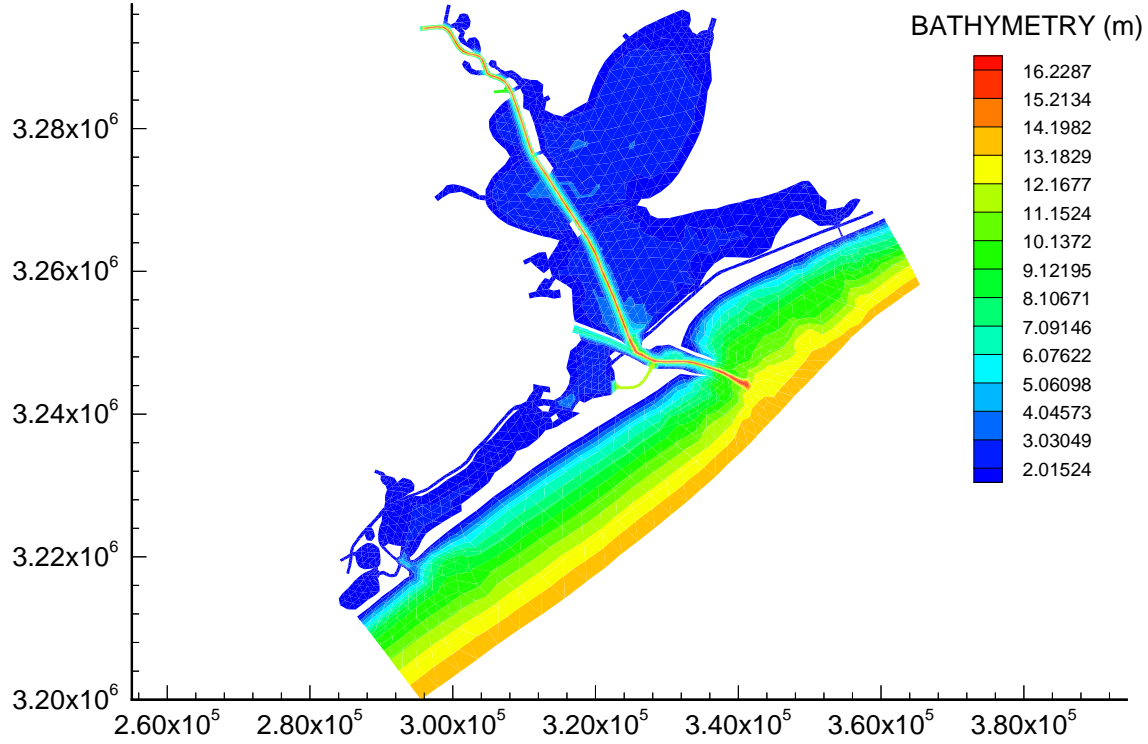
Fig. 5. Galveston Bay: bathymetry. Lengths shown are in meters.

7 Acknowledgments

The authors thank J. J. Westerink and W. G. Gray, as well as the Waterways Experiment Station for sharing the ADCIRC code and various data sets.

References

[1] Brezzi, F., and Fortin, M., 1991. *Mixed and hybrid finite element methods*, Springer-Verlag, New York.

[2] Cerco, C. F., and Cole, T. 1995. "User's Guide to the CE-QUAL-ICM Three-Dimensional Eutrophication Model, Release Version 1.0," Technical Report EL-95-15, U.S. Army Engineer Waterways Experiment Station, Vicksburg, MS.

[3] Chapman, R. S., Gerald, T., and Dortch, M. S. 1996. "Development of Unstructured Grid Linkage Methodology and Software for CE-QUAL-ICM,"
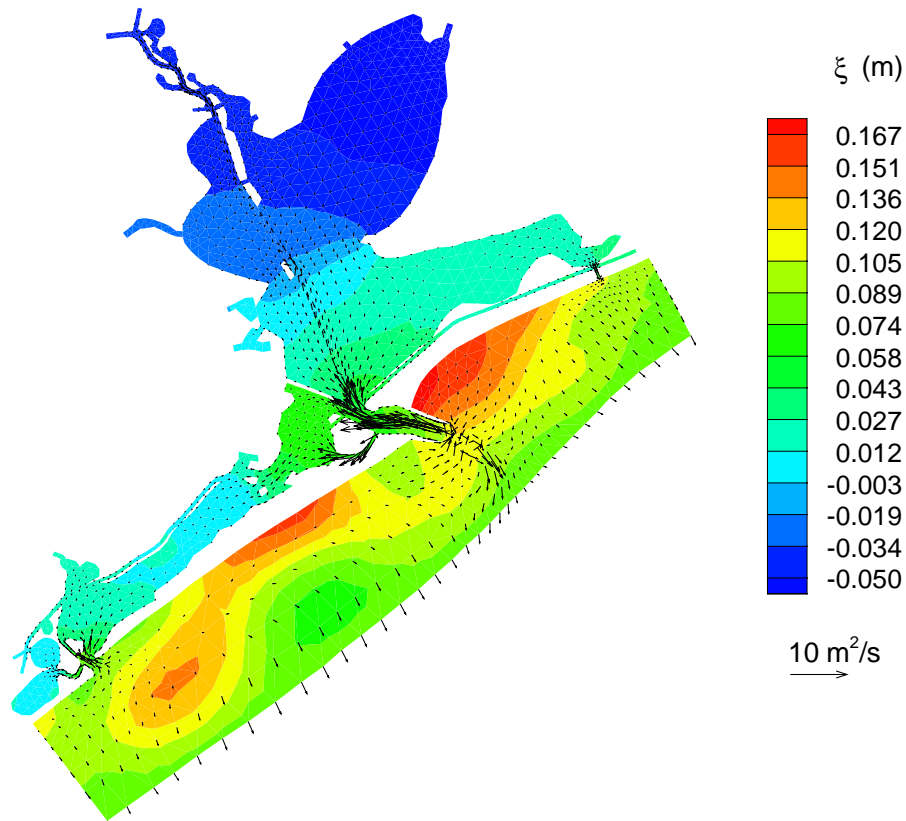
Fig. 6. Galveston Bay: ADCIRC solution at the end of 12 days.

private communication.

[4] Chippada, S., Dawson, C. N., Martínez, M. L., and Wheeler, M. F., "Finite Element Approximations to the System of Shallow Water Equations, Part I: Continuous Time A Priori Error Estimates," *SIAM Journal on Numerical Analysis*, To appear.

[5] King, I. P., and Norton, W. R., 1978. "Recent application of RMA's finite element models for two-dimensional hydrodynamics and water quality." in *Finite Elements in Water Resources II*, C. A. Brebbia, W. G. Gray, and G. F. Pinder, eds., Pentech Press, London.

[6] Kolar, R., Gray, W. G., and Westerink, J. J., 1996. "Boundary conditions in shallow water models- An alternative implementation for finite element codes," *Int. J. Num. Methods in Fluids*, **22**, No.7, pp.603-618.

[7] Lynch, D. R., and Gray, W., 1979. "A wave equation model for finite element tidal computations," *Comput. Fluids*, **7**, pp.207-228.
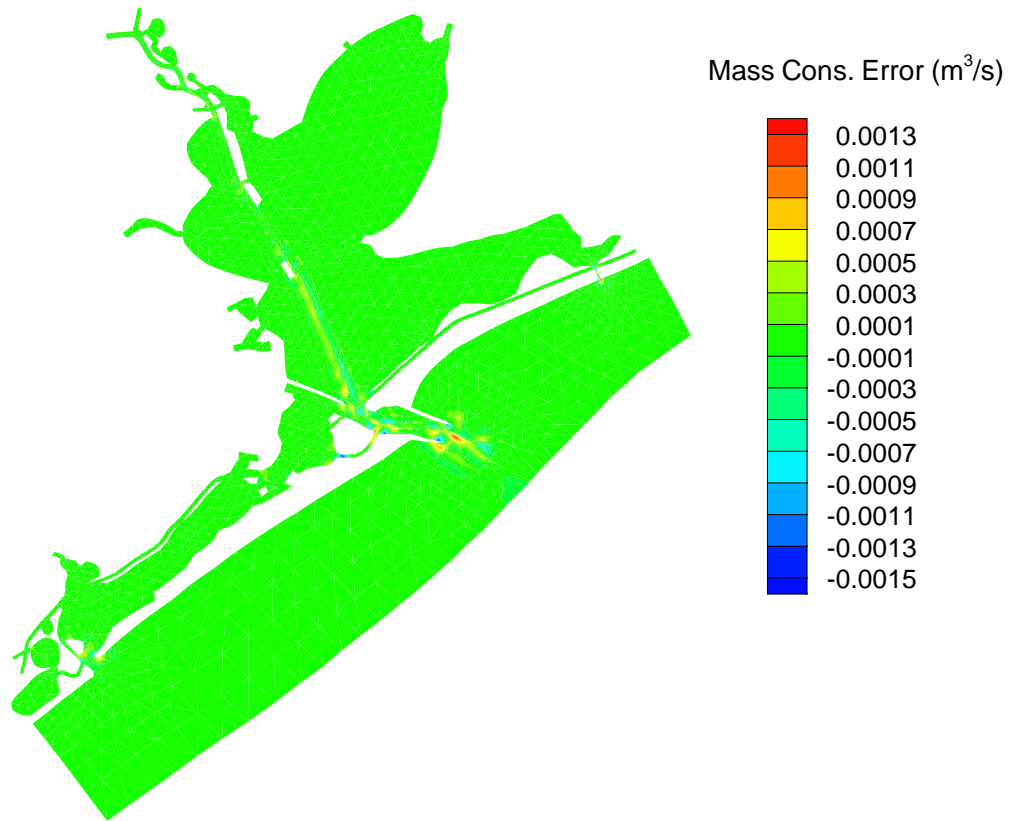
Fig. 7. Galveston Bay: local mass conservation error.

[8] Luettich, Jr., R. A., Westerink, J. J., and Scheffner, N. W., 1991. "ADCIRC: An Advanced Three-Dimensional Circulation Model for Shelves, Coasts and Estuaries," *Report 1, U.S. Army Corps of Engineers*, Washington, D.C. 20314-1000, December 1991.

[9] Norton, W. R., King, I. P., and Orlob, G. T. 1973. "A Finite Element Model for Lower Granite Reservoir," *Water Resource Engineers, Inc.*, Walnut Creek, CA.

[10] Raviart, R. A., and Thomas, J. M., 1977. "A mixed finite element method for 2nd order elliptic problems," *Mathematical Aspects of the Finite Element Method*, Lecture Notes in Mathematics, Springer-Verlag, New York, vol.606, pp.292-315.

[11] Weiyan, T., 1992. *Shallow Water Hydrodynamics*, Elsevier Oceanography Series, 55, Elsevier, Amsterdam.

Pseduo-pressure (m^3/s)

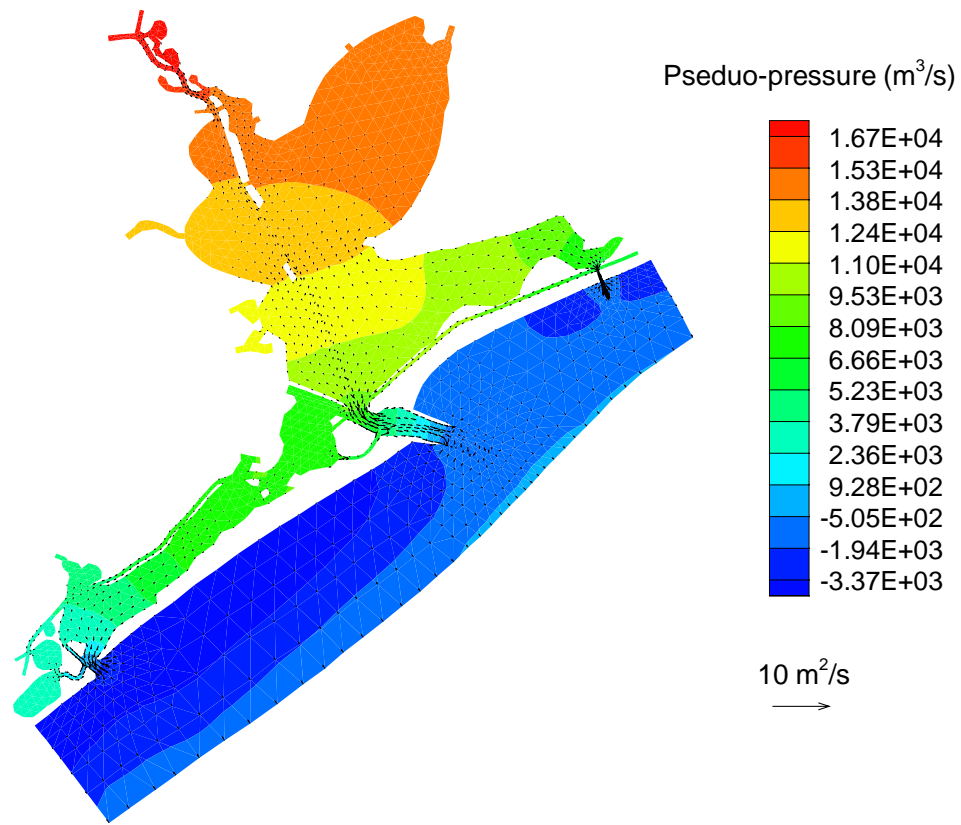| |
|---|
| 1.67E+04 |
| 1.53E+04 |
| 1.38E+04 |
| 1.24E+04 |
| 1.10E+04 |
| 9.53E+03 |
| 8.09E+03 |
| 6.66E+03 |
| 5.23E+03 |
| 3.79E+03 |
| 2.36E+03 |
| 9.28E+02 |
| -5.05E+02 |
| -1.94E+03 |
| -3.37E+03 |

10 m^2/s

Fig. 8. Galveston Bay: velocity correction and pseudo-pressure computed from the conservative projection formulation.